Materials Physics and Mechanics. 2023;51(4): 96-106
Research article
http://dx.doi.org/10.18149/MPM.5142023_9

Submitted: April 16, 2023
Approved: May 8, 2023
Accepted: June 27, 2023

Gas phase large-scale synthesis of Silicon carbide nanowires by industrial electron accelerator

S.P. Bardakhanov [1] ✉, D.Y. Trufanov [1], I.K. Chakin [2], V.R. Gaponenko [1]

[1] Khristianovich Institute of Theoretical and Applied Mechanics of the Siberian Branch of the Russian Academy of Sciences, Novosibirsk, Russia

[2] Budker Institute of Nuclear Physics of the Siberian Branch of the Russian Academy of Sciences, Novosibirsk, Russia

✉ bard@itam.nsc.ru

Abstract. This study focuses on the development of a novel and simple catalyst-free one-stage gas phase synthesis process at atmospheric conditions for silicon carbide based nanomaterials. A mixture of high-purity quartz sand and graphite powder is heated as in air as under argon flow at atmospheric pressure using an industrial accelerator of nominal power 100 kW with a relativistic electron beam of continuous action. The carbothermal reduction reaction of silica occurs and micro granular hexagonal silicon carbide powder produced along with cubic phase SiC nanowires (SiCNWs) for different combinations of the process parameters. The mechanism of the formation of SiCNWs under gas flow is proposed, where Si nanoparticles act as an origin for the SiCNWs grow. The observed productivity shows that the process can be used for the large-scale production of high quality SiC nanowires as well as nano and micro powders of SiC.

Keywords: silica; carbon; silicon carbide; nanowires; SiCNWs; industrial electron accelerator

Acknowledgements. *Authors are grateful to the Russian Foundation for Basic Research and Novosibirsk Region Government for their support (Grant number 19-43-540013), and V. R. Gaponenko also acknowledges support of this work within the state assignment of Ministry of Science and Higher Education of the Russian Federation.*

Citation: Bardakhanov SP, Trufanov DY, Chakin IK, Gaponenko VR. Gas phase large-scale synthesis of Silicon carbide nanowires by industrial electron accelerator. *Materials Physics and Mechanics*. 2023;51(4): 96-106. DOI: 10.18149/MPM.5142023_9.

Introduction

For over a hundred years now, beginning with the Acheson process [1], the carbothermal reduction of silica has been the most widely used method for the synthesis of bulk silicon carbide (SiC) and following production of SiC-based materials at huge industrial scale. Bulk SiC exhibits many preeminent characteristics, including super high hardness and outstanding mechanical robustness, exceptional chemical inertness and corrosion resisting, high melting point (decomposition), low thermal expansion coefficient and excellent thermal stability, suitability for preparation of excellent ceramics, high electron mobility, the last feature is especially useful for highly reliable industrial semiconductor devices.

With regard to obtaining special morphological forms of silicon carbide, the synthesis of SiC nanoparticles started with the nanotechnology era. This trend intensively develops since low dimensionality, quantum confinement and shape effects of SiC nanoparticles demonstrate

Publisher: Peter the Great St. Petersburg Polytechnic University

properties that bulk counterpart cannot possess, what leads to different prospective applications. Respectively, special efforts are devoted to the development of facile methods for the large scale production with cheap raw materials [2,3]. Note, that the gas-phase techniques like plasma synthesis [4,5] and chemical vapor deposition [6], with decomposition of various siloxanes and silanes, are frequently used to produce ultra-small SiC nanoparticles. One can also mention pulsed-laser ablation in liquids [7], but its productivity is not very high.

The growth of elongated whisker-like SiC materials has been a research focus for 50 years now [8,9]. Since the beginning of the 1990s, SiC wires of submicron diameter have been produced using several methods, including the carbothermal reduction of silica [10]. And at the end of the twentieth century, the synthesis of SiC nanowires (SiCNWs) has attracted considerable attention owing to their importance in basic scientific research as well as their potential technological applications [11–13]. The number of papers in this area is about of three hundred now. The availability of large volumes of SiCNWs can lead to immense progress in advanced applications, including photocatalysts, electronics such as emitters, transistors, and sensors, thermal and photoelectric applications, etc.

To date, a variety of methods, both conventional (e.g., carbothermal reduction of silica) and unconventional, used for SiCNW production have been reported [8]. Based on published studies, it can be concluded that most of these methods require the use of expensive raw materials, catalysts, and sophisticated techniques. Additionally, only a few of these studies have reported the synthesis of relatively large quantities of SiCNWs. For instance, the confined reaction method was used for the initial synthesis of carbon nanotubes (CNTs), and the productivity of SiCNWs was 2 g per batch of 15 min [14]. However, the full procedure also included the preparation of a Fe/Ni catalyst and the growth of the CNTs for 1 h. In another study which employed a SiO carbothermal reduction approach using carbon black, relatively specific materials (SiO was commercial and carbon black was treated by arc-discharge plasma for the porosity), were used in 1-h experiments in high-frequency induction furnace, and it was possible to produce 200 g of SiCNWs per day [15]. Other study demonstrated the possibility of synthesizing 3.5 g of SiCNWs within 7 h using expandable graphite (EG) and silicon powder [16]. As the sample of the great efforts to increase the productivity, one could mention the paper [17].

Current research on SiCNWs has been summarized in a recently published book, which highlights the different mechanisms by which SiCNWs can be produced directly from raw materials in the vapor state via the vapor-liquid-solid (VLS) and/or vapor-solid (VS) routes [13]. And in very recent paper [18] it is noted again, that the most of existing methods involve environmentally corrosive and toxic chemicals, or complicated multistep reactions, resulting in much environmental pollution and low efficiency of nanoscale SiC synthesis in a large scale. So, the production of large quantities of high quality SiCNWs using more controllable, predictable, and facile processes is still challenging [13]. Therefore, it is essential to develop a rapid, low-cost, eco-friendly and sustainable preparation strategy for SiC nanowires.

It looks like the carbotermal reduction nowadays could be the most promising base for the large scale production of SiC nanostructures, including SiCNWs. Then the effective heater is necessary to use for this purpose. For our case, it is the electron beam.

It is not widely known, but the electron beam guns are extensively used as concentrated energy source in various material processing applications [19], including welding [20], drilling [21], generation of metal vapor for isotope purification process [22,23] and physical vapor deposition [24]. Therefore, the electron beam is a useful thermal energy source in surface modification, cladding, surfacing, rapid prototyping, engraving as well as texturing, thin film metal and ceramics coating, e.g. [25] preparation technique.

If to say just about welding industry, there are no statistics available to show exactly how many electron beam welding machines are in use worldwide. But it is estimated that the total number of electron beam welding machines is about 3500 in the whole world [21]. Owing to their industrial applications, metal melting and evaporation with e-beam or laser beam systems has been studied extensively in literature, e.g. [26–29].

To emphasize the nanotechnology applications, besides film deposition with nanocrystals [30], the electron beam evaporation (EBE, as with continuous as pulsed beam) is used for high entropy alloys [31], nanoparticles' production [32,33]. In fairness, the papers [34,35] should be noted, where to the best of our knowledge, the first attempt was made to purposefully obtain a noticeable amount of oxide nanopowders using electron beam evaporation. But they used the installation of only 1 kWt with a voltage in the range 15 to 30 kV and oxygen at a pressure of 7 Pa.

But in spite of widespread electron beam technologies, all of them had a serious disadvantage in the sense of large scale production of nanomaterials. The usual energy produced range was not more than 400 keV. Therefore, previous commercial EBE could be used only at vacuum environment or in low-pressure gas, mostly not more than 100 Pa. At non vacuum conditions, the energy of the electrons scatters by gas molecules, and the electron beam without enough energy cannot be used as the powerful heater. In 80s this barrier had been override by introducing the new kind of industrial accelerator developed by Budker Institute of Nuclear Physics with focused electron beam extracted into atmosphere [36]. And we employ this facility since 1992 for the gas phase synthesis of nanomaterials [37–39].

Further, a critical analysis is the following of the pros and cons of our electron beam heating method. Actually, it is almost fully copied from very recent paper [40] of our colleagues. And this analysis compares the laser beam and electron beam heating.

Laser cladding is considered to be an effective process for the fabrication of different coatings. This technology has such advantages as high power density, beam focusing accuracy, and perfect beam position control. At the same time, the laser cladding technology also has a number of disadvantages, such as a low efficiency coefficient and a low depth of radiation penetration, which make it difficult to obtain cladded layers of considerable thickness.

The electron beam as an energy source seems to be an attractive alternative to a laser for applications in cladding technologies. Traditional electron beam processing is carried out in vacuum chambers at a beam energy of 20–400 keV. Around 90 % of the electron beam energy is absorbed by the metals, which is one of the main advantages of the electron beam, especially taking into account that the absorption of the laser radiation may be as low as 3-7 %. However, a convenient electron beam treatment has a number of limitations. Firstly, the processing of large surfaces is quite complicated since the treated items must be placed in a vacuum chamber. The other disadvantage is the relatively small penetration depth of electrons into the material due to the relatively low electron beam energy. For instance, the maximum penetration depth of electrons with an energy of 200 keV in Ti is 0.13 mm, and for electrons with an energy of 400 keV, it reaches 0.66 mm.

The non-vacuum electron beam cladding technology is free of the aforementioned disadvantages. High-energy electron accelerators developed by Budker Institute of Nuclear Physics provide high-power electron beams with an energy of 1.4 MeV. A specially designed vacuum system allows for the direct injection (without any foil) of the electron beams in the air wth atmospheric pressure. Due to the high initial energy, electrons penetrate the material to a depth of about 2 mm (for Ti and other elements with similar atomic numbers), which provides rapid heating of the surface layer [36]. Note, that for the evaporation purpose laser beam is less suitable due to scattering on high concentration vapor, and its efficiency strongly depends on treated target material. The high energy electron beam is free of such disadvantages. As for the gas phase production of nanomaterials (nanoparticles, nanopowders), in difference with

vacuum conditions, such facility allows fully independent control of electron beam power and gas transportation through the evaporation region at arbitrary flow rate in surrounding atmospheric pressure.

Therefore, this study aims at developing a novel and facile catalyst-free one-stage process for the production of large quantities of coarse SiC and SiCNWs powders by employing carbothermal reduction via the vaporization of a mixture of high purity quartz sand (silica) and high purity graphite (carbon) using for the first time an industrial accelerator acting at atmospheric pressure with continuous gas flow.

Methods

The high purity quartz sand and high purity graphite powder were mixed in the ratio of 1:2. Industrial accelerator ELV-6, having a power of 100 kW and a relativistic electron beam with initial energy 1.4 MeV, was used as continuous beam source. This energy value provides a 5 m path in the 101.325 kPa (1 atm) air pressure until the energy is completely dissipated. The scheme of accelerator is presented at Fig. 1. The scale 5 meters denotes the approximate total height of accelerator together with under-beam equipment. H1, H2, H3 are the sections of differential pumping separating inner high vacuum from the outer atmospheric pressure. Notation D is the local electron beam diameter at the certain distance from the accelerator outlet. Design details can be found in paper [40].

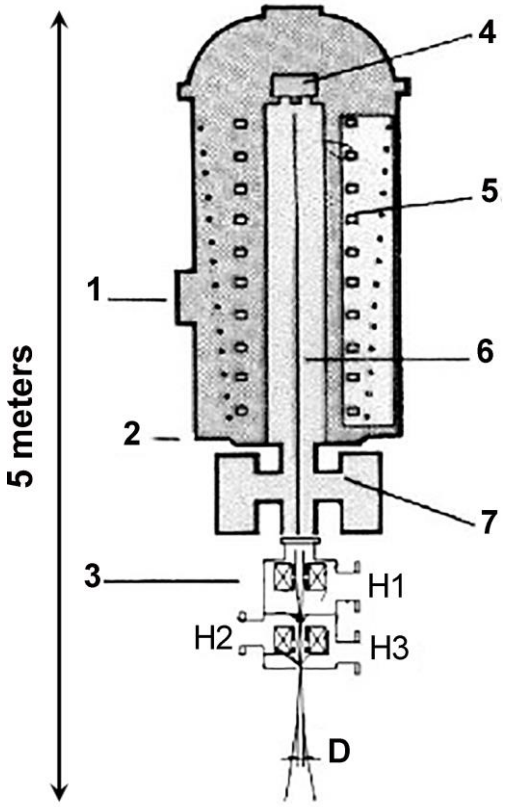

Fig. 1. The scheme of the ELV-6 electron beam accelerator: 1 – power supply system, 2 –water cooling system, 3 – focused beam release system, 4 – electron gun, 5 – high-voltage rectifier, 6 – accelerating tube, 7 – magnetic discharge pumps, D – local diameter of electron beam

A unique feature of this equipment is the ability to inject a narrow beam directly into the atmosphere, thus, offering the possibility of heating rate more than a thousand degree per second and easy vaporization of any material at normal pressure, in difference with other

electron beam technologies which usually require vacuum in the treatment chamber. It leads to another advantage, consisting of continuous gas flow control independently of electron beam power. Production of nanopowders from raw materials in the gas phase, including the semi-industrial scale (that is still in operation since 2005 with the yield more than 7 kg h^{-1} at 70 kW for the silica nanopowder) have been reported [37–39]. The measured dependence of yield versus electron beam power is exponential, for instance, at 100 kW it is about 30 kg h^{-1}.

In this study, a medium-size treatment chamber (sublimator) was used. The detailed scheme of facility used for the nanopowder production is presented at Fig. 2. It has been discussed in a previous study [41]. The raw mixture was loaded into the sublimator. The sublimator is a water-cooled closed stainless-steel cylinder into which an electron beam can be injected through a 2 mm diameter hole at the top. The gas passes through sublimator and together with condensed nanoparticles moves along the gas path to filter that capture fine powders.

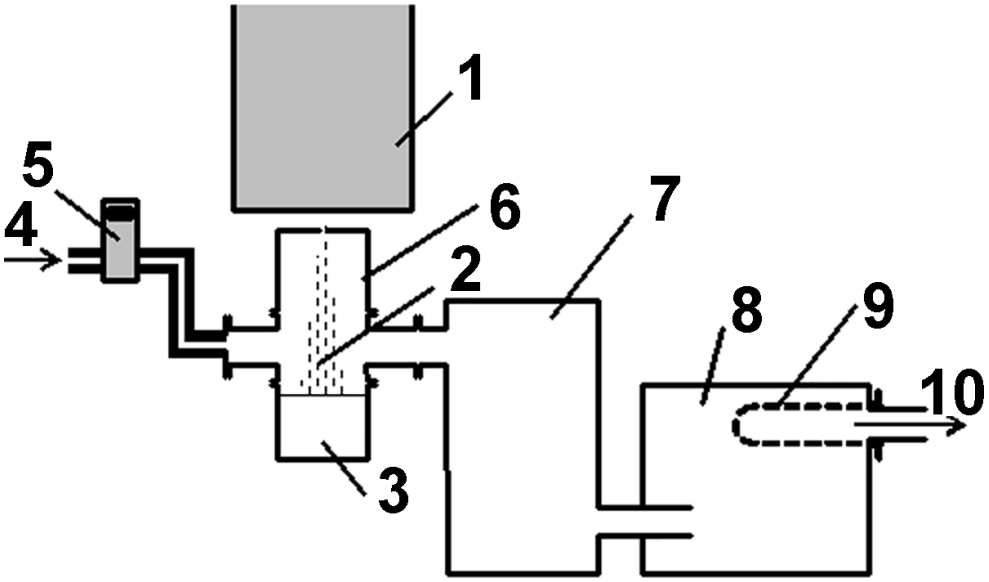

Fig. 2. The scheme of experimental path: 1 - electron accelerator; 2 - electron beam down from accelerator; 3 – target material; 4 – carrier gas supply channel; 5 – electronic flow regulator; 6 – water-cooled sublimator; 7 – coarse fraction separator; 8 – plastic box; 9 – fabric bag filter; 10 – outlet of carrier gas

The series of experiments involved the treatment of the SiO_2/C mixture with forced argon blowdown at a gas flow rate of 12 L min^{-1} with a beam power of 6 kW. The specific surface area of the powders was measured by Brunauer-Emmett-Teller (BET) method. X-ray diffraction (XRD, Bruker D8 Advance New X-ray diffractometer) and transmission electron microscopy (JEM-2200FS, JEOL Ltd.) with energy-dispersive spectroscopy (EDS) were used for the detailed analysis of the nanomaterials.

Results and Discussion

The pattern of the substance inside the sublimator after experiment is illustrated in Fig. 3. TEM and EDS showed that powder 1, deposited in the region surrounding the beam exposure zone 2, and filament 3, which formed above the heated region, consisted of light-brown, fluffy, and amorphous silicon monoxide (SiO). They condensed from the corresponding vapor resulting from the high-temperature reaction that occurred when the SiO_2/C mixture was heated by the electron beam.

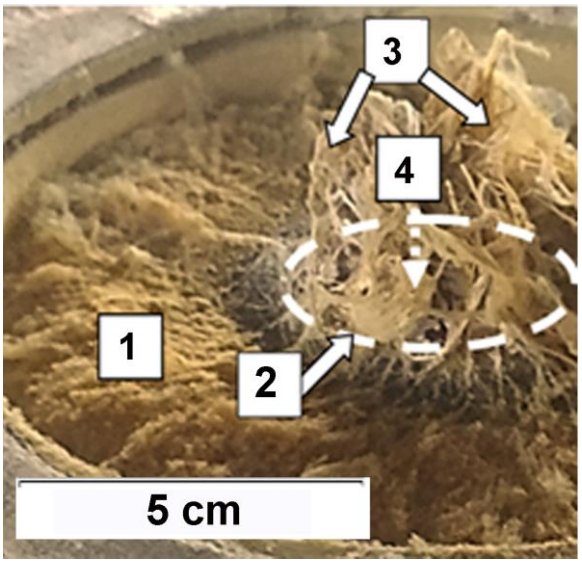

Fig. 3. Pattern of the deposited substance in the sublimator at beam power of 6 kW. 1, zone outside of electron beam; 2, electron beam heating zone; 3, silicon monoxide filaments; 4, electron beam direction

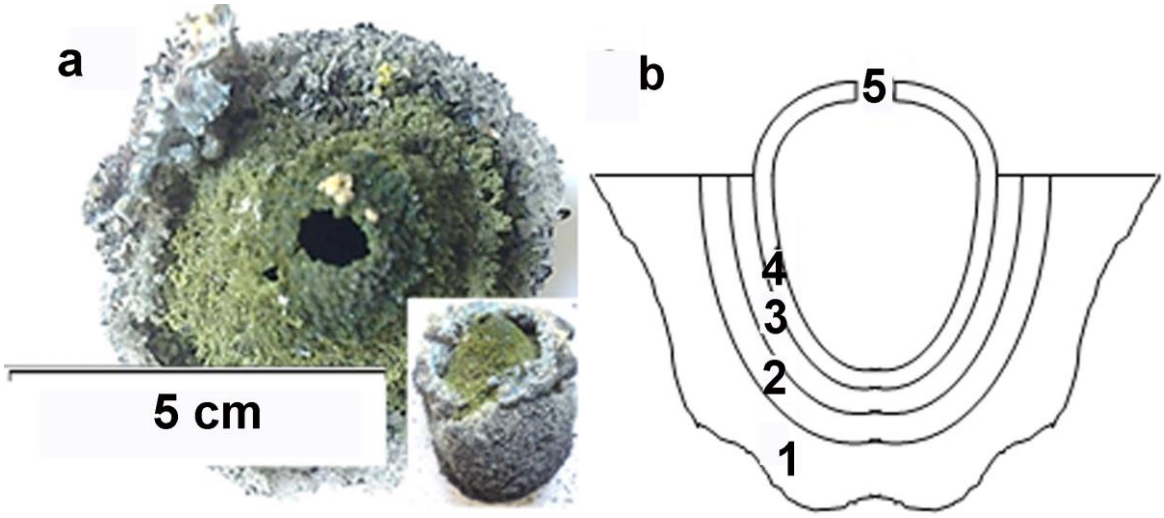

Fig. 4. Egg-like structure: (a) top view (Inset: Typical side view);
(b) scheme of internal structure: 1, surrounding raw mixture; 2, sintered layer of quartz sand with graphite; 3, porous black-gray uniform layer of melted silica and carbon;
4, green shell of closed cavity; 5, electron beam entry

The region of exposure close to the center of the sublimator (indicated by arrow 4) had a special structure. Figure 4 shows an egg-like structure that was excavated from the heated area (zone 2, Fig. 3). The top view of the egg-like structure (main field of Fig. 4(a)) revealed its average diameter to be ~60 mm. At the center, a hole with diameter within the range of 10–15 mm, representing the point of entry of the electron beam, was observed. The average height of the whole egg-like structure (Inset, Fig. 4(a)) was ~70 mm. The internal texture of the egg-like structure is presented in Fig. 4(b). It reveals the presence of constituent layers, of which layer 4 (green shell) was highly porous and could easily be transformed into a microscopic powder. This powder consisted of approximately 100 % of SiC hexagonal 6H α structure (JSPDS No. 42–1360).

The powders collected further downstream in the parts of the whole installation (e.g. filter) had a very fluffy texture, and were green-brown in color. The results showed that the samples typically had a specific surface area of ~100 m^2 g^{-1}, and X-ray analysis revealed that they consisted of cubic SiC (JSPDS No. 29–1129). Figure 5(a) shows that the powder predominantly consisted of smoothly curved and entangled rods with diameter in the range of ~ 15–30 nm, and the magnified image of Fig. 5(b) established the "nanocables". EDX spectra also revealed that the inner nanorods consisted of Si and C with the atomic ratio 1:1. The outer cover consists of amorphous silica.

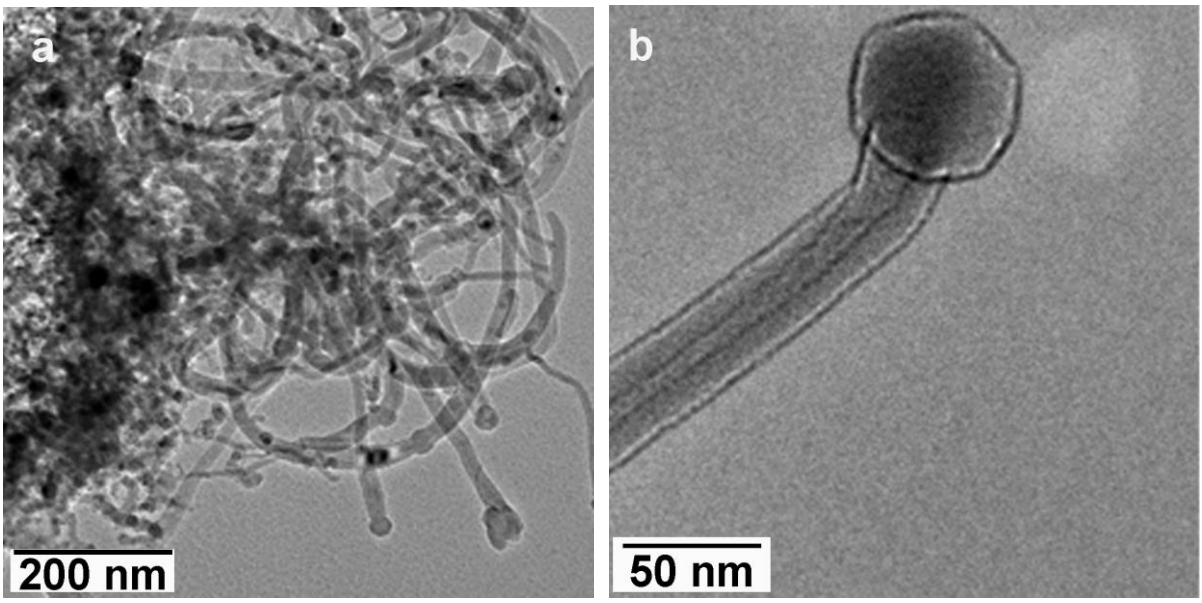

Fig. 5. Species morphology of nanowires:
(a) general view of nanowires; (b) single silicon nanoparticle integrated with SiCNW

In all the samples, free silicon was present as nanoparticles. Firstly, as shown in Fig. 5(b), they appeared as a nanocable head, and secondly, a smaller proportion appeared as relatively detached silicon nanoparticles. Electron-diffraction pattern of them, usually interpreted in the literature as nanocrystalline silicon.

Based on the results of this study, a possible mechanism that highlights a few key events associated with the production of SiCNW has been proposed for the carbothermal reduction under powerful electron beam treatment. Equations (1) and (2) represent solid to vapor reactions that occurred inside the egg-like structure owing to the heating effect of the electron beam:

$$SiO_{2(s)} + C_{(s)} \rightarrow SiO_{(g)} + CO_{(g)} \quad , \qquad (1)$$

$$C_{(s)} \rightarrow C_{(g)}. \qquad (2)$$

Equations (3) and (4) represent the solid-to-liquid and liquid-to-vapor reactions.

$$SiO_{2(s)} + 2C_{(s)} \rightarrow Si_{(l)} + 2CO_{(g)} \qquad (3)$$

$$Si_{(l)} \rightarrow Si_{(g)} \qquad (4)$$

Layer 4 of the egg-like structure (Fig. 2(b)) was possibly formed according to Equations (5) and (6), resulting in the deposition of hexagonal SiC.

$$SiO_{(g)} + 3CO_{(g)} \rightarrow SiC_{(s)} + 2CO_{2(g)} \qquad (5)$$

$$SiO_{(g)} + 2C_{(g)} \rightarrow SiC_{(s)} + CO_{(g)} \qquad (6)$$

The Equation (3) is a well-known overall reaction for the industrial production of silicon by carbothermal reduction in big furnaces. The resulting quantity of liquid Si (which is usually collected from the bottom of the furnace as a target product) depends on the initial ratio of SiO_2

and C. The industrial process also results in production of large quantities of SiO according to Equation (1).

In this study, some quantities of Si and CO were also produced. As for the elementary Si, the results of our earlier studies showed that pure silicon ingots can easily be melted and evaporated by the electron beam according to Equation (4), and with subsequent cooling in inert gases, it is possible to produce large quantities of silicon nanopowders composed of nanoparticles covered by a thin layer of amorphous silica [42]. In this study, we assume that the reduced silicon in liquid phase in the bottom of the egg-like structure, is vaporized by the electron beam.

At the electron beam exposition, the carbon can be evaporated with a large yield of condensed carbon substance [36]. Therefore, Equation (2) yields gaseous carbon. Thus, the generation of SiO, Si, CO and C (as sources of Si and C) is possible in our process.

In this study, the SiC nanorods were not observed inside egg-like structures. This suggests that SiC nanorods originate in the outer gaseous flow. In the flowing argon environment, $SiO_{(g)}$ and $CO_{(g)}$ interacted according to Equation (5) and possibly according to Equation (6) as well, forming SiC precursors. Silicon vapor was also generated from the heated zone, and it was considered that in the cooling atmosphere, the solidifying silicon nanoparticles resulting from Equation (4) acted as a catalyst, providing a surface on which SiCNWs grew in the gas stream. The similar supposition was made in paper [43]. The same conjecture was reported for the formation of some quantities of SiC nanorods for the specific ratio SiO_2/CH_4H at the thermal plasma synthesis [44]. We suppose that more recent papers [45-47] also support the probability of topochemical reactions at the surface of solidifying silicon nanoparticles.

The potential yield of SiCNWs could be estimated, based on our current and previous results. The total productivity G was about 0.2 kg h^{-1} for 6 kW of electron beam power P. Assuming that the function G(P) was linear, the productivity would have been ∼3 kg h^{-1} at P = 100 kW. Instead, an exponential relationship was observed when an electron beam was used as a heater, at correspondent scaling the yield would be higher than 5 kg h^{-1}.

Conclusions

In this study, we have proposed a novel and simple catalyst-free one-stage process for synthesis of SiCNWs through carbothermal reduction reaction that employs the relativistic electron beam of a high-power industrial accelerator at atmospheric pressure. The process is continuous and allows the independent control of power and gas flow. The mechanism of SiCNWs formation under gas flow is proposed according to which the SiCNWs grow originates on the Si nanoparticles.

References

1. Acheson G. *Carborundum*. US492767 (Patent) 1893.
2. Beke D, Valenta J, Karolyhazy G, Lenk S, Czigany Z, Markus BG, Kamaras K, Simon F, Gali A. Room-temperature defect qubits in ultrasmall nanocrystals. *J. Phys. Chem. Lett*. 2020;11(5): 1675–1681.
3. An Z, Xue J, Cao H, Zhu C, Wang H. A facile synthesis of silicon carbide nanoparticles with high specific surface area by using corn cob. *Advanced Powder Technology*. 2019;30(1): 164–169.
4. Czosnek C, Bucko MM, Janik JF, Olejniczak Z, Bystrzejewski M, Labedz O, Huczko A. Preparation of silicon carbide SiC-based nanopowders by the aerosol-assisted synthesis and the DC thermal plasma synthesis methods. *Materials Research Bulletin.* 2015;63: 164–172.
5. Wang C, Zhou J, Song M, Chen X, Zheng Y, Yang C, Xia W, Xia W. Fabrication of ultra-small SiC nanoparticles with adjustable size, stoichiometry and photoluminescence by AC multi-arc plasmas. *Ceramics International.* 2022;48: 632–641.

6. Liu R, Liu M, Chang J. Large-scale synthesis of monodisperse SiC nanoparticles with adjustable size, stoichiometric ratio and properties by fluidized bed chemical vapor deposition. *J. Nanopart. Res.* 2017;19: 26.
7. Zhu J, Hu S, Wang W, Xia W, Chen H, Chen X. Luminescent amorphous silicon carbide ultrafine nanoparticles fabricated by pulsed-laser ablation. *Appl. Phys. A*. 2017;123: 244.
8. Prakash J, Venugopalan R, Tripathi BM, Ghosh SK, Chakravartty JK, Tyagi AK. Chemistry of one dimensional silicon carbide materials: Principle, production, application and future prospects. *Prog. Solid State Chem*. 2015;43: 98–122.
9. Li X, Liu Q, Chen S, Li W, Liang Z, Fang Z, Yang W, Tian Y, Yang Y. Quasi-aligned SiC@C nanowire arrays as free-standing electrodes for high-performance micro-supercapacitors. *Energy Storage Mater*. 2020;27: 261–269.
10. Liang J, Guo W, Liu J, Qin H, Gao P, Xiao H. Synthesis of in-situ SiC nanowires by self-assembly nanoparticles on carbon fibers and their photoluminescence properties. *J. Alloys and Compd*. 2019;797: 101–109.
11. Meng GW, Zhang LD, Qin Y, Mo CM, Phillipp F. Synthesis of beta-SiC nanowires with SiO2 wrappers. *Nanostruct. Mater*. 1999;12: 1003–1006.
12. Yang P, Yan R, Fardy M. Semiconductor Nanowire: What's Next? *Nano Lett.* 2010;10(5): 1529–1536.
13. Chen S, Li W, Li X, Yang W. Silicon carbide nanowires and electronics. In: Shen G, Chueh YL. (eds.) *Nanowire Electronics: Nanostructure Science and Technology*. Singapore: Springer; 2019. p.237–335.
14. Chiu SC, Li YY. SiC nanowires in large quantities: Synthesis, band gap characterization, and photoluminescence properties. *J. Cryst. Growth*. 2009;311(4): 1036–1041.
15. Wang FL, Zhang LY, Zhang YF. SiC nanowires synthesized by rapidly heating a mixture of SiO and arc-discharge plasma pretreated carbon black. *Nanoscale Res Lett*. 2009;4: 153–156.
16. Chen J, Shi Q, Xin L, Liu Y, Liu R, Zhu X. A simple catalyst-free route for large-scale synthesis of SiC nanowires. *J. Alloys and Compd*. 2011;509(24): 6844–6847.
17. Li ZJ, Yu HY, Song GY, Zhao J, Zhang H, Zhang M, Meng AL, Li QD. Ten-gram scale SiC@SiO2 nanowires: high-yield synthesis towards industrialization, in situ growth mechanism and their peculiar photoluminescence and electromagnetic wave absorption properties. *Phys. Chem. Chem. Phys.* 2017;19 (5): 3948–3954.
18. Yang B, Sun R, Li X, Ma M, Zhang X, Wang Z, Yi W, Zhang Z, Yang R, Sun H, Gao G, Chu Y, Zhao Z, Liu X. Rapid fabrication of hierarchical porous SiC/C hybrid structure: toward high-performance capacitive energy storage with ultrahigh cyclability. *J. Mater. Sci*. 2021;56 16068–16081.
19. Kumar VD, Mazumder A, Alangi N, Mukherjee J, Sethi S. Evaluation of crucible for cold hearth transverse electron beam vapor generator. *Case Studies in Thermal Engineering*. 2021;27: 101318.
20. Węglowski MS, Blacha S, Phillips A. Electron beam welding–techniques and trends–review. *Vacuum*. 2016;130: 72–92.
21. Leitz KH, Koch H, Otto A, Alexander M, Lower T, Schmidt M. Numerical simulation of drilling with pulsed beams. *Physics Procedia*. 2012;39: 881–892.
22. Anklam TM, Berzins LV, Hagans KG, George K, McClelland M.A, Scarpetti RD, Shimer DW. Uranium AVLIS vaporizer development. In: *Proc. SPIE 1859, Laser Isotope Separation 1993*. 1993. p.277–286.
23. Greenland PT. Laser isotope separation. *Contemp. Phys*. 1990;31(6): 405–424.
24. Singh J, Wolfe D. Review Nano and macro-structured component fabrication by electron beam-physical vapor deposition (EB-PVD). *J. Mater. Sci*. 2005;40: 1–26.

25. Oks EM, Tyunkov AV, Yushkov YG, Zolotukhin DB. Ceramic coating deposition by electron beam evaporation. *Surface and Coatings Technology.* 2017;325(25): 1–6.
26. Powell A, Pal U, Avyle JVD, Damkroger B, Szekely J. Analysis of multicomponent evaporation in electron beam melting and refining of titanium alloys. *Metall. Mater. Trans. B.* 1997;28(6): 1227–1239.
27. Klassen A, Forster VE, Juechter V, Körner C. Numerical simulation of multi-component evaporation during selective electron beam melting of TiAl. *Journal of Materials Processing Technology*. 2017;247: 280–288.
28. Zhao Y, Aoyagi K, Yamanaka K, Chiba A. Role of operating and environmental conditions in determining molten pool dynamics during electron beam melting and selective laser melting. *Additive Manufacturing.* 2020;36: 101559.
29. Amine T, Newkirk JW, Lioua F. An investigation of the effect of direct metal deposition parameters on the characteristics of the deposited layers. *Case Studies in Thermal Engineering.* 2014;3: 21–34.
30. Efremova SL, Salatov AV, Kulikova DP, Kasyanov AA, Bykov IV, Afanasev KN, Tananaev PN, Baryshev AV. On the fabrication of one-dimensional magnetophotonic crystals from various oxides and metal–organic decomposition-made Bi0.5Y2.5Fe5O12. *Journal of Physics D: Applied Physics*. 2021;54(50): 505305.
31. Ustinov AI, Polishchuk SS, Demchenkov SA, Melnychenko TV, Skorodzievskii VS. Formation of thin foils of high-entropy CrFeCoNiCu alloys by EB-PVD process. *Surf. Coat. Technol.* 2020;403: 126440.
32. Sokovnin SY, Il'ves VG, Zuev MG. Production of complex metal oxide nanopowders using pulsed electron beam in low-pressure gas for biomaterials application. In: Grumezescu AM. (ed.) *Engineering of Nanobiomaterials. Applications of Nanobiomaterials*. 2016;2: 29–75.
33. Ilves VG, Gaviko VS, Malova OA, Murzakaev AM, Sokovnin SY, Uimin MA, Zuev MG. Phase transformation in vacuum and basic physicochemical properties of heterophasic amorphocrystalline Bi2O3-based nanopowder produced by pulsed electron beam evaporation. *Journal of Alloys and Compounds*. 2021;881: 160514.
34. Ramsay JDF, Avery RG. Ultrafine oxide powders prepared by electron beam evaporation. Part 1 Evaporation and condensation processes. *Journal of Materials Science.* 1974;9: 1681–1688.
35. Ramsay JDF, Avery RG. Ultrafine oxide powders prepared by electron beam evaporation. Part 2 Powder characteristics. *Journal of Materials Science* 1974;9: 1689–1695.
36. Fadeev SN, Golkovski MG, Korchagin AI, Kuksanov NK, Lavruhin AV, Petrov SE, Salimov RA, Vaisman AF. Technological applications of BINP industrial electron accelerators with focused beam extracted into atmosphere. *Radiation Physics and Chemistry*. 2000;57(3–6): 653–655.
37. Lukashov VP, Bardakhanov SP, Salimov RA, Korchagin AI, Fadeev SN, Lavruhin AV. *A way to obtain the ultrafine silica powder, device for its realization and ultrafine silica powder*. RU2067077 (Patent) 1994.
38. Bardakhanov SP. The formation of fine silica powder after vaporization of quartz. In: *Proc. 5th Int. Conf. Computer Aided Design of Adv. Materials and Technologies (CADAMT'97), Baikal Lake, Russia*. 1997. p.88–89. (In-Russian)
39. Bardakhanov SP, Korchagin AI, Kuksanov NK, Lavrukhin AV, Salimov RA, Fadeev SN, Cherepkov VV. Nanopowder production based on technology of solid raw substances evaporation by electron beam accelerator. *Mater Sci Eng B.* 2006;132: 204–208.
40. Ruktuev AA, Golkovski MG, Lazurenko DV, Bataev VA, Ivanov IV, Thommes A, Bataev IA. Ti–Ta–Nb clads produced by electron beam surface alloying in regular air at

atmospheric pressure: Fabrication, structure, and properties. *Materials Characterization*. 2021;179: 111375.
41. Zavjalov AP, Zobov KV, Chakin IK, Syzrantsev VV, Bardakhanov SP. Synthesis of copper nanopowders using electron-beam evaporation at atmospheric pressure of inert gas. *Nanotechnologies in Russia.* 2014;9: 660–666.
42. Efremov MD, Volodin VA, Marin DV, Arzhannikova SA, Goryainov SV, Korchagin AI, Cherepkov VV, Lavrukhin AV, Fadeev SN, Salimov RA, Bardakhanov SP. Visible photoluminescence from silicon nanopowders produced by silicon evaporation in a high-power electron beam. *JETP Lett.* 2004;80: 544–547.
43. Latu-Romain L, Ollivier M, Mantoux A, Auvert G, Chaix-Pluchery O, Sarigiannidou E, Bano E, Pelissier B, Roukoss C, Roussel H, Dhalluin F, Salem B, Jegenyes N, Ferro G, Chaussende D, Baron T. From Si nanowire to SiC nanotube. *J. Nanopart. Res.* 2011;13: 5425–5433.
44. Ramachandran M, Reddy RG. Thermal plasma synthesis of SiC. *Adv. Manuf.* 2013;1: 50–61.
45. Kukushkin, SA, Osipov AV. Phase equilibrium in the formation of silicon carbide by topochemical conversion of silicon. *Phys. Solid State.* 2016;58: 747–751.
46. Grashchenko AS, Kukushkin SA, Osipov AV, Redkov AV. Formation of composite SiC-C coatings on graphite via annealing Si-melt in CO. *Surface and Coatings Technology*. 2021;423: 127610.
47. Kukushkin SA, Osipov AV. Thermodynamics, kinetics, and technology of synthesis of epitaxial layers of silicon carbide on silicon by coordinated substitution of atoms, and its unique properties. A review. *Condensed Matter and Interphases.* 2022;24(4): 407–458.

THE AUTHORS

Bardakhanov S.P.
e-mail: bard@itam.nsc.ru

Trufanov D.Y.
e-mail: trufanov@itam.nsc.ru

Chakin I.K.
e-mail: chak_in2003@bk.ru

Gaponenko V.R.
e-mail: vasko-nsk@yandex.ru